# 3D-Microstructure Modeling and Performance Evaluation for Solid Oxide Fuel Cell (MIEC) Cathodes

Bernd Rüger[*,1], André Weber[1] and Ellen Ivers-Tiffée[1]
[1]Universität Karlsruhe (TH), Institute of Materials for Electrical Engineering (IWE)
*Corresponding author: Adenauerring 20b, 76131 Karlsruhe, bernd.rueger@iwe.uni-karlsruhe.de

**Abstract:** Mixed electronic/ ionic conducting (MIEC) cathode materials are qualified for the application in intermediate temperature SOFCs. The area specific resistance of MIEC cathodes is likewise determined by chemical composition and microstructure.
A three-dimensional finite element method model, which is capable to analyze and predict the performance of MIEC cathodes, was developed. Representations for the actual cathode microstructure are automatically generated according to characteristic measures like cathode thickness, composition, porosity and average particle size. The model calculates the spatial distributions of the oxygen activity, the diffusive oxygen flux in the pores as well as the ionic current density inside the MIEC-cathode and inside the electrolyte material. Based on these values the area specific resistance of the cathode and the penetration depth of the ionic current can be evaluated.
This paper will analyze the effect of surface-exchange $k_O$ and bulk diffusion coefficient $D_O$ as well as the influence of microstructure properties on the cathode performance.

**Keywords:** SOFC, modeling, cathodes, microstructure

## 1. Introduction

Mixed ionic/ electronic conducting (MIEC) materials i.e. $La_{0.6}Sr_{0.4}Co_{0.2}Fe_{0.8}O_3$ (LSCF) are qualified for the application as cathode in intermediate temperature solid oxide fuel cells (IT-SOFC). The reduction of oxygen molecules from the gas phase and the incorporation of oxygen ions into the electrolyte is not limited to the three phase boundary (gas/ electrode/ electrolyte) but at best extended to the entire volume of the cathode structure according to the specific values of surface-exchange coefficient $k_O$ and bulk diffusion coefficient $D_O$. As a consequence, at a specific current density the area specific cathode resistance $ASR_{cat}$ of a MIEC cathode is considerable small compared to purely electron conducting cathodes, i.e. $La_{0.75}Sr_{0.2}MnO_3$ (LSM).

Besides the material composition, which determines surface exchange $k_O$ and bulk diffusion coefficient $D_O$, the $ASR_{cat}$ is determined by electrode microstructure. A model-based estimation of characteristic measures like cathode thickness, porosity and average particle size is highly desirable. One-dimensional models apply statistical parameters (porosity $\varepsilon$, tortuosity $\tau$ and inner surface area $a$) to describe the three-dimensional cathode microstructure [1]. Appropriate statistical parameters can be calculated by the percolation theory on the condition that the cathode microstructure is treated as being composed by sintered spheres [2; 3]. The one-dimensional models are suitable for the calculation of the penetration depth of the ionic conduction part in MIEC cathodes and in Ni/YSZ cermet anodes.

In this work a model for MIEC cathodes is presented which includes a three-dimensional representation for the cathode microstructure. The processes occurring in the model are calculated spatially resolved with the finite element method (FEM). In this approach the microstructure parameters (cathode thickness, particle size and porosity) and their influence is modeled explicitly and is not only described by statistical parameters. A similar model was already used to examine cermet Ni/YSZ anode microstructures and presented in [4]. An FEM model like the one presented here basically allows evaluating arbitrary microstructures and geometries. But there are restrictions in respect to memory size and calculation time taken into consideration.

## 1. Model

### 1.1 Processes

The processes (i) gas diffusion, (ii) surface exchange, (iii) bulk diffusion and (iv) charge

transfer depicted in Fig. 1 are taken into account in the model at a constant temperature $T$ and a constant pressure $p$. Four boundary conditions are given: oxygen partial pressure on the anode and cathode side ($p_{GC}$, $p_{CE}$) as well as the potentials of the electrodes ($\Phi_{MIEC}$, $\Phi_{CE}$). According to equation [4] the electrode potential of the cathode $\Phi_{MIEC}$ contains all voltage losses $\eta_{Model}$ occurring in the model. At $\eta_{Model} = 0$ V the current $I = 0$ A, whereas with increasing $\eta_{Model}$ values the current $I$ in the model is created.

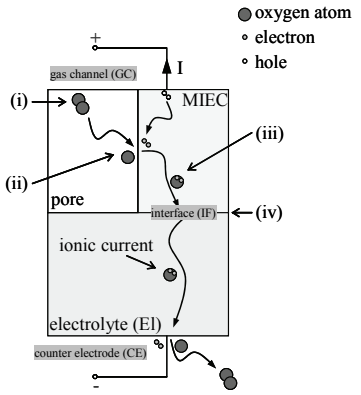


**Figure 1**. Illustration of the processes (i) gas diffusion, (ii) surface exchange, (iii) bulk diffusion and (iv) charge transfer, which are included in the presented three-dimensional model. All processes are described by the molar fraction of oxygen $x_{O2}$ (in the gas phase), the oxygen ion concentration $c_O$ (in the MIEC) and the electric potential $\Phi_{El}$ (in the electrolyte)

The area specific cathode resistance $ASR_{cat}$ is calculated as a characteristic measure for the MIEC cathode performance. In a first step the current $I$ is determined by integration of the current density. This allows to calculate the area specific resistance of the model $ASR_{Model} = \eta_{Model} / I{\cdot}A$. Because the electrolyte length $l_{el}$ and the ionic conductivity $\sigma_{El}$ of the electrolyte are known a subtraction of the ideal area specific electrolyte resistance $ASR_{El} = l_{el} / \sigma_{El}$ is possible. Altogether this gives the area specific cathode resistance $ASR_{cat} = ASR_{Model} - ASR_{El}$. The influence of current constriction in the electrolyte is in contrast to one-dimensional models taken into account by the model. This additional loss is attributed to the $ASR_{cat}$.

### 1.2 Equations, Parameters and Boundary Conditions

Gas diffusion: The gas phase is treated as a binary mixture of oxygen and nitrogen. At the gas channel a constant molar fraction of oxygen $x_{O2,GC}$ is given by the oxygen partial pressure $p_{GC}$. According to the dusty-gas-model [5] the diffusion of oxygen molecules in the pores of the cathode to the electrochemically active faces is modelled by

$$N_{O_2} = -\frac{p}{RT}\nabla x_{O_2} \cdots \cdots \left[\frac{1-\left(1-\sqrt{M_{O_2}/M_{N_2}}\right)x_{O_2}}{D_{O_2N_2}} + \frac{1}{D_{O_2}^{K}\left(d_P\right)}\right]^{-1} \quad (1)$$

This approach takes the interaction of oxygen molecules with the pore walls into account via the Knudsen diffusion coefficient $D_K$, which is dependent on the pore radius. The diffusion coefficient $D_{O2N2}$ is calculated after Fuller [6]. The equation further depends on temperature $T$, ideal gas constant $R$ and the molar masses $M_i$. Note: comparing results with and without gas diffusion showed in the cases treated here a negligible influence of the gas diffusion on the $ASR_{cat}$.

Surface exchange: Oxygen is exchanged through the boundary faces between gas phase and MIEC material. Without a current the oxygen ion concentration in the MIEC material reaches an oxygen partial pressure dependent equilibrium value $c_{O,eq}$ [3]. This concentration is decreasing under current load ($c_O < c_{O,eq}$) and there is a oxygen flow through the boundary

$$\vec{n} \cdot N_{O_2} = -k_O \cdot \left(c_{O,eq} - c_O\right)/2 \quad (2)$$

$$\vec{n} \cdot j_{diff} = k_O \cdot \left(c_{O,eq} - c_O\right) \quad (3)$$

The surface-exchange coefficient $k_O$ is oxygen partial pressure as well as temperature dependent. A constant $k_O$ value is used in the simulations as the temperature is assumed to be constant and as the oxygen partial pressure in the pores is hardly changing.

Bulk diffusion: Due to the high electron conductivity a constant electrical potential is assumed throughout the MIEC material

$$\Phi_{MIEC} = U_{Nernst}\left(p_{GC}, p_{CE}\right) + \Phi_{CE} - \eta_{Model} . \quad (4)$$

Thus movement of oxygen ions in the MIEC material is solely determined by bulk diffusion

$$\nabla \cdot j_{diff} = \nabla \cdot \left(-D_O \nabla c_O\right) = 0 . \quad (5)$$

The bulk diffusion coefficient $D_O$ is oxygen partial pressure and temperature dependent too. In the simulations a constant $D_O$ value is used as the temperature is assumed to be constant and as the dependence on the oxygen partial pressure is small (3).

Charge transfer: Oxygen ions are exchanged at MIEC material/electrolyte interfaces (IF). The local charge transfer voltage

$$\begin{aligned} \eta_{ct} &= U_{Nernst,IF} - \left(\Phi_{MIEC} - \Phi_{El,IF}\right) \\ &= \eta_{Model} - \eta_{MIEC} - \eta_{El} \end{aligned} \quad (6)$$

$$U_{Nernst,IF}\left(p_{MIEC,IF}, p_{CE}\right) = \ldots$$

$$\ldots \frac{RT}{2F} \cdot \log\left(\sqrt{\frac{p_{MIEC,IF}}{p_{CE}}}\right) \quad (7)$$

depends on the local difference in the chemical potential ($U_{Nernst,IF}$) and on the difference in the electrical potential between electrolyte $\Phi_{El,IF}$ and MIEC material $\Phi_{MIEC.}$ The partial pressure $p_{MIEC,IF}$ in the MIEC material at the interface is being calculated and corresponds to the partial pressure with which the MIEC material would be in equilibrium due to the local oxygen ion concentration $c_{O,IF}$ at the interface [3]. With this voltage the local oxygen ion exchange current density can be determined by

$$j_{ct} = \frac{\eta_{ct}}{ASR_{CT}} \quad (8)$$

$$\vec{n} \cdot j_{diff} = \frac{j_{ct}}{2 \cdot F} \quad (9)$$

$$\vec{n} \cdot j_{curr} = j_{ct} . \quad (10)$$

The area specific charge transfer resistance $ASR_{CT}$ is the only parameter for which no values can be found in literature. If a LSCF/CGO (Gd-doped CeO2) material system is considered a (close to) lossless charge transfer can be assumed [3]. The charge transfer resistance for other material combinations like LSCF/YSZ (Y-doped ZrO2) can be substantially higherand dominate the cathode resistance due to e.g. insulating secondary phases (lanthanides and zirconates). A very small value $ASR_{CT}$ = 0.1 mΩcm² is used but a use of higher values is also possible.

Ionic current: A constant chemical potential determined by $p_{CE}$ is being assumed in the electrolyte, because the oxygen ion concentration is approximately independent of oxygen partial pressure and because of the ideal reversible counter electrode used. Thus Oxygen ions in the electrolyte are moving because of a gradient in electrical potential

$$\nabla \cdot j_{curr} = \nabla \cdot \left(-\sigma_{El} \nabla \Phi_{El}\right) = 0 . \quad (11)$$

Again $\sigma_{El}$ denotes the ionic conductivity of the electrolyte.

Counter electrode: As an ideal reversible counter electrode is chosen at this boundary $\Phi_{El,CE} = \Phi_{CE}$ and $p_{El,CE} = p_{CE}$, holds whereas $\Phi_{CE} = 0$ is set in the model.

### 1.3 Geometry

Cathode structures with a significant percentage of porosity (20 to 40%) are of major importance for the technical application in solid oxide fuel cells. In Fig. 2 an approximation for the microstructure of porous cathodes is depicted. On top of the cathode structure there is a current collector ($l_{cc}$ = 0.5 µm) and underneath there is an electrolyte. Object of the electrolyte and the current collector is collection and distribution of current and/or gas to the partially porous cathode structure respectively. For the presented three-dimensional model a comparatively small electrolyte length of $l_{el}$ = 5 µm was proven to be adequate to take into account current constriction in the electrolyte. The cathode microstructure is approximated by equally sized cubes with edge length $l_{cu}$, which are aligned symmetrically as depicted in Fig. 2. Cubes are randomly assigned to be (i) electrolyte material, (ii) MIEC material (in accordance with material composition) or (iii)

of empty space, taking into account porosity. Overall only a limited number of cubes (i.e. $N_x = 7$, $N_y = 7$ and $N_z = 48$ cubes (in short, 7x7x48 model)) respectively area can be taken into account by the model. According to recently presented evaluations for cermet based Ni/YSZ anodes the calculated results are increasingly falsified with smaller areas and it was shown that an area of 7x7 cubes delivers reliable results [4].

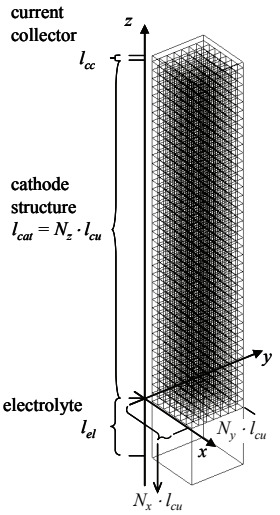


**Figure 2**. In the three-dimensional model the underlying cathode microstructure is approximated by $N_x$x$N_y$x$N_z$ equally sized and symmetrically aligned cubes. An example with $N_x = 7$, $N_y = 7$ and $N_z = 40$ cubes (in short, 7x7x40 model) is given. Each cube is assigned to be (i) electrolyte material, (ii) MIEC material or (iii) represents a pore.

### 1.4 Implementation

The model is implemented as a collection of m-files and can be run from the command line of COMSOL Script or MATLAB. The modeling process is divided into four fully automated parts:

(i) Geometry Generation: In this part the geometry of the model is generated and saved to disk.

(ii) Mesh Generation: In this part generated geometries are loaded and meshs with automated settings ("Normal") are calculated. Hereby the mesh is refined twice and all three meshs (initial mesh, refined and double refined) are saved to disk.

(iii) Material Distribution Generation: In this part the material distributions are generated. Generating and saving material distributions. Using saved material distributions instead of generating them on the fly during simulations allows for better comparability. A material distribution is saved as a matrix of size $N_x$x$N_y$x$N_z$. Prime numbers are used as entries, whereby each prime represents one kind of material (e.g. 2 represents MIEC material). The use of prime numbers eases selection of appropriate boundary conditions during simulation.

(iv) Simulation and Postprocessing: The simulation can be started from the command line but for most of the simulations comsolbatch was used (This is beneficial as memory gets freed). For the simulations some parameters are varied in a batch file and unchanged parameters were collected in a parameter file. Simulation was done by a function which performed the following steps:

a. Parameters are handed over
b. Mesh file is loaded
c. Most Important: Equations and Boundary Conditions are set according to the material distribution.
d. Simulation is performed
e. Postprocessing is conducted
f. Simulation results (only postprocessed values) are stored.

The structure of the code allows for efficient simulations as the time consuming steps of generating geometry and mesh are done only once for each parameter set. Still part (iv) takes between one and ten and in average three minutes depending on parameters.

## 2. Results

SOFC cathode structures with technical relevance require electrocatalytic activity, chemical and structural compatibility to the interfaces (electrolyte and interconnector), as well as excellent values for performance and long term stability. Therefore cathode structures, regardless of whether pure electronic or mixed

ionic-electronic conducting (MIEC) materials are introduced, possess a minimum porosity (> 20%) as well as a minimum thickness (> 20 µm) (nanoscaled interlayers of MIEC materials are not taken into account). In our approach, this type of MIEC cathode is modeled with a three-dimensional replication of the microstructure. First results presented here are based on a $l_{cat}$ = 30 µm thick MIEC cathode composed of particles with a size of $l_{cu}$ = 750 nm and a volumetric composition of 65 vol-% MIEC material and 35 vol-% porosity.

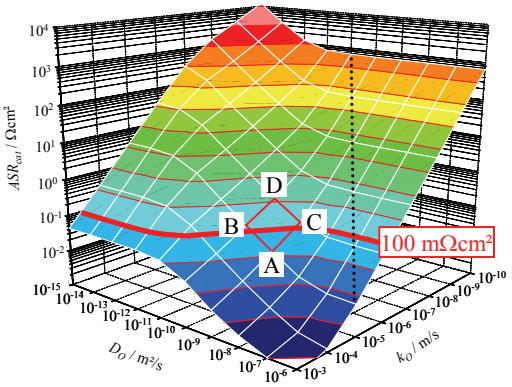


**Figure 3**. The area specific cathode resistance $ASR_{cat}$ at 800 °C averaged from 30 simulations is depicted dependent on bulk diffusion $D_O$ and surface exchange coefficient $k_O$. A 7x7x40 model was used with a porosity of 35 vol-%, a cathode thickness $l_{cat}$ of 30 µm and a cube length $l_{cu}$ of 750 nm.
($T$ = 800 °C, $\sigma_{El}$ = 4.72 S/m, $\eta_{Model}$ = 0.1 V, $ASR_{CT}$ = 0.1 mΩcm², $p$ = 1 bar, $p_{GC}$ = 0.21 bar, $p_{CE}$ = $10^{-23}$ bar)

## 2.1 Variation of Material Parameters $k_O$ and $D_O$

The area specific cathode resistance $ASR_{cat}$ at 800 °C is depicted in Fig. 3 as a function of material parameters $k_O$ and $D_O$. As expected, the calculated characteristic map of the $ASR_{cat}$ can be divided into three regions:

(i) For small $k_O$-values (right of the dotted line) the $ASR_{cat}$ is surface controlled (cp. control of current in oxygen membranes [9]), the diffusion within the material is rather fast and the $ASR_{cat}$ is solely determined by the value of $k_O$.

(ii) In the area left hand to the dotted line, both surface exchange $k_O$ and diffusion coefficient $D_O$ determine the $ASR_{cat}$ on an equal base, therefore the $ASR_{cat}$ increases with decreasing $k_O$ and $D_O$ values.

(iii) For the third case, where $k_O$ is very large and $D_O$ is very small, only a minor impact of $D_O$ can be found due to a favourable incorporation of oxygen at the triple phase boundary (corresponding to a short diffusion length).

The area specific cathode resistance $ASR_{cat}$ is given in table 1 for four different hypothetical MIEC materials (A, B, C, D) and for a measured LSCF cathode [8]. Compared to the material parameters from [3; 7] the $ASR_{cat}$ values of hypothetical material A and LSCF are in fair agreement.

**TABLE I.** The area specific cathode resistance $ASR_{cat}$ at 800 °C given for four different cathodes of hypothetical types of MIEC material (A, B, C, D) and for a measured LSCF cathode [8]. A 7x7x40 model with a porosity of 35 % and a cube length of 750 nm was used.
($T$ = 800 °C, $\sigma_{El}$ = 4.72 S/m, $\eta_{Model}$ = 0.1 V, $ASR_{CT}$ = 0.1 mΩcm², $p$ = 1 bar, $p_{GC}$ = 0.21 bar, $p_{CE}$ = $10^{-23}$ bar)

| Material | $k_O$ / m/s | $D_O$ / m²/s | $ASR_{cat}$ / mΩcm² |
|---|---|---|---|
| A | $10^{-5}$ | $10^{-9}$ | 38 |
| B | $10^{-5}$ | $10^{-10}$ | 121 |
| C | $10^{-6}$ | $10^{-9}$ | 124 |
| D | $10^{-6}$ | $10^{-10}$ | 373 |
| LSCF | $1.51 \cdot 10^{-5*}$ | $7.24 \cdot 10^{-10*}$ | > 15 |

* value derived from [3;7]

## 2.2 Average Ionic Current Density

The presented three-dimensional model provides the current density distribution in the overall volume of the porous MIEC cathode structure. Evaluation of the average ionic current density $j_{diff,z}$ allows for optimization of cathode thickness. The average ionic current density $j_{diff,z}$ is calculated by integration of the ionic current density in $z$-direction in cross-sectional plane parallel to the $xy$-plane at a given z-position.

The average ionic current density $j_{diff,z}$ in the MIEC material A increases from zero at the cathode surface to the total current density of 2.06 A/cm² at the interface MIEC cathode/ electrolyte as shown in Fig. 4. A variation of $k_O$ and $D_O$, according to B,C and D in table 1, results in (i) different total current densities at the interface MIEC cathode/electrolyte as a starting point, as well as in (ii) distinctively shaped curves within the penetrated porous MIEC cathode volume. It should be noticed that for MIEC material B and C, where $k_O$ is large

and $D_O$ is small respectively $k_O$ is small and $D_O$ is large, the same total current density is calculated for the interface MIEC cathode/electrolyte, but the spatial distribution in $z$-direction differs noticeably.

For MIEC material B ($k_O = 10^{-5}$ m/s and $D_O = 10^{-10}$ m²/s) an entire cathode thickness $l_{cat}$ of 10 µm would be sufficient, whereas MIEC material C ($k_O = 10^{-6}$ m/s and $D_O = 10^{-9}$ m²/s) the cathode thickness $l_{cat}$ of 30 µm is still insufficient. Without doubt, the three-dimensional model presented here already provides information required for the selection of the "optimum" thickness $l_{cat}$ of a MIEC cathode as a function of $k_O$ and $D_O$.

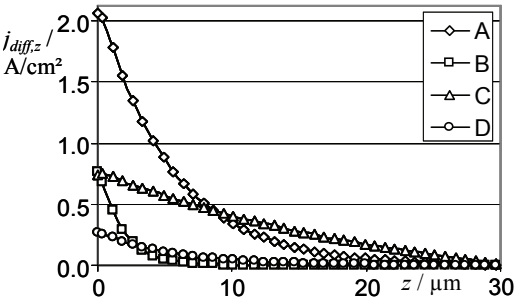


**Figure 4**. The ionic current density in the cathode structure $j_{diff,z}$ at 800 °C averaged from 30 simulations for 4 different types (A, B, C, D see table 1) of porous MIEC cathodes is depicted. The penetration depth of the ionic current density $j_{diff,z}$ (z-direction from electrolyte into the cathode volume) depends significantly on MIEC material parameters bulk diffusion $D_O$ and surface exchange coefficient $k_O$. A 7x7x40 model was used with a porosity of 35 vol-%, a cathode thickness $l_{cat}$ of 30 µm and a cube length $l_{cu}$ of 750 nm.
($T$ = 800 °C, $\sigma_{El}$ = 4.72 S/m, $\eta_{Model}$ = 0.1 V, $ASR_{CT}$ = 0.1 mΩcm², $p$ = 1 bar, $p_{GC}$ = 0.21 bar, $p_{CE} = 10^{-23}$ bar)

### 2.3 Variation of the Particle Size

The presented model is not only capable to calculate the $ASR_{cat}$ as a function of material parameters but also as a function of particle size, as the cube length $l_{cu}$ can be varied. This is examined for a porous cathode of hypothetical material A with a constant cathode thickness $l_{cat}$ of 12 µm. The volumetric composition of 65 vol-% MIEC material and 35 vol-% porosity was kept constant. The area specific cathode resistance $ASR_{cat}$ at 800 °C is depicted in Fig. 5 dependent on cube size $l_{cu}$. The $ASR_{cat}$ decreases with decreasing particle size (cube length $l_{cu}$) thus leading to an improvement of the $ASR_{cat}$ by a factor of ≈ 2 by decreasing the particle size from 1 µm to 250 nm.

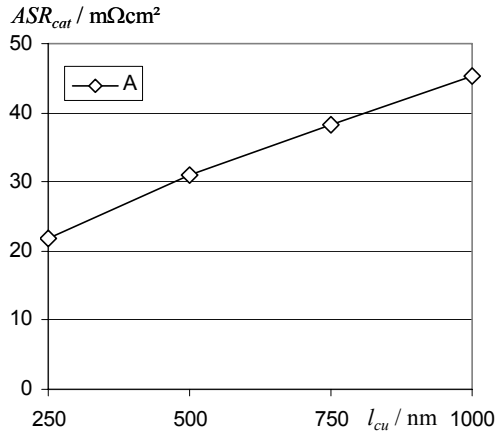


**Figure 5**. The area specific resistance $ASR_{cat}$ at 800 °C averaged for 30 simulations for a porous cathode of hypothetical material A (see table 1) is depicted dependent on cube length $l_{cu}$. Four models (7x7x12, x16, x24, x48) were used with a porosity of 35 vol-%, and a cathode thickness $l_{cat}$ of 12 µm.
($T$ = 800 °C, $\sigma_{El}$ = 4.72 S/m, $\eta_{Model}$ = 0.1 V, $ASR_{CT}$ = 0.1 mΩcm², $p$ = 1 bar, $p_{GC}$ = 0.21 bar, $p_{CE} = 10^{-23}$ bar)

## 3. Conclusion

The FEM based three-dimensional model presented allows for the calculation of approximate values for the area specific resistance $ASR_{cat}$ of a porous MIEC cathode with a variation in $k_O$, $D_O$, particle size (cube length $l_{cu}$) and thickness $l_{cat}$. Cathode microstructure is approximated by equally sized and symmetrically aligned cubes. Cubes can be occupied either by MIEC material, electrolyte material or pores. The model considers (i) gas diffusion in the pores, (ii) oxygen exchange between gas phase and mixed conductor, (iii) oxygen ion diffusion in the mixed conductor and ohmic losses in the electrolyte. The transport of oxygen ions across the MIEC cathode/ electrolyte interface (iv) is covered by an area specific resistance.

The area specific resistance $ASR_{cat}$ of a set of MIEC cathode candidates has been examined at

800 °C in a vast parameter range for the model parameters $k_O$ and $D_O$. As expected the $ASR_{cat}$ decreases with increasing parameters $k_O$ and $D_O$. For $La_{0.6}Sr_{0.4}Co_{0.2}Fe_{0.8}O_3$ material parameters values have been identified for $k_O$ and $D_O$ from literature [3; 7]. A comparison of measurement and simulation yields a fair correspondence [8].

In contrast to one-dimensional models, current constrictions in the transport paths are taken into account. Compared to the treatment of electrode microstructure with effective parameters it is possible to set up more complex electrode microstructures in the finite element method.

The model is only capable of taking into account a small number of cubes (i.e. the calculations based on the presented 7x7x40 model consists of 1960 individual cubes). Therefore only a restricted number of microstructures, cathode thicknesses and cube lengths can be simulated. Furthermore there are issues with the precision of the results because only a limited resolution of the FEM mesh was possible. In future the modeled processes will be regarded in more details, e.g. it is planned to take into account oxygen partial pressure dependence of the values for $k_O$ and $D_O$. Moreover the geometry generator is to be extended to generate structures closer to reality, i.e. it is planned to introduce spherical particles instead of cubes.

## 4. References


[1] S. B. Adler, J. A. Lane, and B. C. H. Steele, *J. Electrochem. Soc.*, **143**, 3554 (1996).

[2] J. H. Nam and D. H. Jeon, *Electrochimica Acta*, **51**, 3446 (2006).

[3] M. Søgaard, P. V. Hendriksen, T. Jacobsen, M. Mogensen, *Proc. 7th European SOFC Forum*, B064 (2006).

[4] B. Rüger, A. Weber, D. Fouquet, E. Ivers-Tiffée, *Proc. 7th European SOFC Forum*, B0705 (2006).

[5] R. Suwanwarangkul, E. Croiset, M. W. Fowler, P. L. Douglas, E. Entchev, M. A. Douglas, *Journal of Power Sources*, **122**, 9 (2003).

[6] A. Schönbucher, Einführung in die Stoffübertragung, Georg Thieme Verlag, (1984)

[7] P. Ried, E. Bucher, W. Preis, W. Sitte and P. Holtappels, *ECS Transactions*, *7* (1) 1217, (2007).

[8] A. Leonide, V. Sonn, A. Weber, E. Ivers-Tiffée, *ECS Transactions*, **7** (1) 521, (2007).

[9] H. J. M. Bouwmeester, H. Kruidhof, and A. J. Burggraaf, *Solid State Ionics*, **72**, 185 (1994).


## 5. Acknowledgements

The authors gratefully acknowledge Prof. W. Sitte and Dr. E. Bucher (Univ. Leoben, Austria) for providing material parameters for LSCF; COMSOL Support for assistance with COMSOL multiphysics 3.3 problems; Dr. Thomas Carraro (Univ. Karlsruhe, Computing Centre) for advice regarding numerical questions and our colleagues André Leonide, Judith Hartmann and Priscila Gonçalves for their support.